J|A|C|S
ARTICLES
Published on Web 07/29/2003

# Formation of Single-Bonded $(C_{60}^-)_2$ and $(C_{70}^-)_2$ Dimers in Crystalline Ionic Complexes of Fullerenes

Dmitri V. Konarev,*[,†,‡] Salavat S. Khasanov,[†,§] Gunzi Saito,*[,†] Akihiro Otsuka,[†,||] Yukihiro Yoshida,[†] and Rimma N. Lyubovskaya[‡]

*Contribution from the Division of Chemistry, Graduate School of Science, Kyoto University, Sakyo-ku, Kyoto 606-8502, Japan, Institute of Problems of Chemical Physics RAS, Chernogolovka, Moscow region 142432 Russia, Institute of Solid-State Physics RAS, Chernogolovka, Moscow region, 142432, Russia, and Research Center for Low Temperature and Materials Sciences, Kyoto University, Sakyo-ku, Kyoto 606-8502, Japan*

Received April 9, 2003; E-mail: konarev@icp.ac.ru; saito@kuchem.kyoto-u.ac.jp

***Abstract:*** New ionic complexes of fullerenes $C_{60}$ and $C_{70}$ with decamethylchromocene $Cp^*_2Cr\cdot C_{60}\cdot(C_6H_4Cl_2)_2$ (**1**), $Cp^*_2Cr\cdot C_{60}\cdot(C_6H_6)_2$ (**2**); the multicomponent complex of $(Cs^+)(C_{70}^-)$ with cyclotriveratrylene $CTV\cdot(Cs)_2\cdot(C_{70})_2\cdot(DMF)_7\cdot(C_6H_6)_{0.75}$ (**3**); bis(benzene)chromium $Cr(C_6H_6)_2\cdot C_{60}\cdot(C_6H_4Cl_2)_{0.7}$ (**4**), $Cr(C_6H_6)_2\cdot C_{60}\cdot C_6H_5CN$ (**5**), $Cr(C_6H_6)_2\cdot C_{70}\cdot C_6H_4Cl_2$ (**6**), $Cr(C_6H_6)_2\cdot C_{60}$ (**7**); cobaltocene $Cp_2Co\cdot C_{60}\cdot C_6H_4Cl_2$ (**8**), $Cp_2Co\cdot C_{70}\cdot(C_6H_4Cl_2)_{0.5}$ (**9**); and cesium $Cs\cdot C_{70}\cdot(DMF)_5$ (**10**) have been obtained. The complexes have been characterized by the elemental analysis, IR-, UV−vis−NIR spectroscopy, EPR and SQUID measurements. It is shown that $C_{60}^{\bullet-}$ exists as a single-bonded diamagnetic $(C_{60}^-)_2$ dimer in **1**, **2**, **4**, **5**, and **8** at low temperatures (1.9−250 K). The dimers dissociate above 160−250 K depending on donor and solvent molecules involved in the complex. $C_{60}^{\bullet-}$ dimerizes reversibly and shows a small hysteresis (<2 K) at slow cooling and heating rates. The single-bonded diamagnetic $(C_{70}^-)_2$ dimers are also formed in **6**, **9**, and **10** and begin to dissociate only above 250−360 K. The IR and UV−vis−NIR spectra of $\sigma$-bonded negatively charged fullerenes are presented.

## Introduction

Ionic compounds of fullerenes are interesting both by their unusual physical properties (superconductivity and ferromagnetism)[1] and a large variety of dimeric and polymeric structures of negatively charged fullerenes.[2] Most of ionic charge transfer (CT) complexes of fullerenes: $TDAE\cdot C_{60}$,[3] $Cp_2Co\cdot C_{60}\cdot CS_2$,[4] $Cp_2Co\cdot C_{60}\cdot C_6H_5CN$,[5] $Cp^*_2Ni\cdot C_{60}\cdot CS_2$,[6] $Cr^{III}TPP\cdot C_{60}\cdot(THF)_3$,[7] various salts of $C_{60}^{n-}$ ($n$ = 1, 2 and 3) with $PPN^+$, $Ph_4P^+$ and others[8] contain monomeric fullerene radical anions.

The linear $C_{60}^-$ polymer bonded by two single bonds (cyclobutane ring) is formed in metallic $M\cdot C_{60}$ phases (M = K, Rb, and Cs).[9] The linear $C_{70}^{2-}$ and $C_{60}^{3-}$ polymers bonded by one single bond were observed in $M\cdot C_{70}\cdot nNH_3$ salts (M = Ca, Sr, and Ba),[10] and in $Na_2RbC_{60}$ and $Li_3CsC_{60}$ phases.[11] A single-bonded linear $C_{60}^-$ polymer was also found in ionic $Cr(C_6H_5Me)_2\cdot C_{60}\cdot CS_2$. The $C_{60}$ anions form linear chains with a 9.6 Å distance between the centers and the shortest $C(C_{60})\cdots C(C_{60})$ distance of 2.12 Å. However, the disorder in the fullerene part does not allow satisfactory characterization of this polymer.[12] $C_{60}^{4-}$ forms a two-dimensional polymer bonded by four single bonds in $Na_4C_{60}$.[13]

The first single-bonded $(C_{60}^-)_2$ dimer was found in metastable $M\cdot C_{60}$ phases (M = K, Rb, and Cs).[14] Azafullerene forms a neutral single-bonded $(C_{59}N)_2$ dimer, which is isoelectronic to $(C_{60}^-)_2$ and has similar properties.[15] A reversible phase transition

† Division of Chemistry, Graduate School of Science, Kyoto University.
‡ Institute of Problems of Chemical Physics RAS.
§ Institute of Solid-State Physics RAS.
|| Research Center for Low Temperature and Materials Sciences, Kyoto University.

(1) (a) Rosseinsky, M. J.*J. Mater. Chem.* **1995**, *5*, 1497−1513. (b) Gotschy, B. *Fullerene Sci. and Technol.* **1996**, *4*, 677−698. (c) Konarev, D. V.; Lyubovskaya, R. N. *Russ. Chem. Rev.* **1999**, *68*, 19−38.
(2) Prassides, K. In *The Physics of Fullerenes-Based and Fullerene-Related Materials*; Andreoni, W., Ed.; Kluwer Academic Publishers: Netherlands, 2000, pp 175−202.
(3) Allemand, P.-M.; Khemani, K. C.; Koch, A.; Koch, A.; Wudl, F.; Holczer, K.; Donovan, S.; Grüner, G.; Thompson, J. D. *Science* **1991**, *253*, 301−303.
(4) Balch, A. L.; Lee, J. W.; Noll, B. C.; Olmstead, M. M. In *Recent Advances in the Chemistry and Physics of Fullerenes and Related Materiales*; Eds. Kadish, K. M.; Ruoff, R. S. **1994**, *24*, 1231−1243.
(5) Stinchcombe, J.; Pénicaud, A.; Bhyrappa, P.; Boyd, P. D. W.; Reed, C. A. *J. Am. Chem. Soc.* **1993**, *115*, 5212−5217.
(6) Wan, W. C.; Liu, X.; Sweeney, G. M.; Broderick, W. E., *J. Am. Chem. Soc.* **1995**, *117*, 9580−9581.
(7) Pénicaud, A.; Hsu, J.; Reed, C. A.; Koch, A.; Khemani, K.; Allemand, P.-M.; Wudl, F. *J. Am. Chem. Soc.* **1991**, *113*, 6698−6670.
(8) (a) Reed, C. A.; Bolskar, R. D. *Chem. Rev.* **2000**, *100*, 1075−1119. (b) Bilow, U.; Jansen, M. *J. Chem. Soc., Chem. Commun.* **1994**, 403−404. (b) Paul, P.; Xie, Z.; Bau, R.; Boyd, P. D. W.; Reed, C. A. *J. Am. Chem. Soc.* **1994**, *116*, 4145−4146.
(9) (a) Stephens, P. W.; Bortel, G.; Faigel, G.; Tegze, M.; Jánossy, A.; Pekker, S.; Oszlanyi, G.; Forró, L. *Nature* **1994**, *370*, 636−639. (b) Winter, J.; Kuzmany, H.; Soldatov, A.; Persson, P.; Jacobsson, P.; Sundqvist, B. *Phys. Rev. B* **1996**, *54*, 17 486−17 492.
(10) (a) Brumm, H.; Peters, E.; Jansen, M. *Angew. Chem., Int. Ed. Engl.* **2001**, *40*, 2069−2071. (b) Wedig, U.; Brumm, H.; Jansen, M. *Chem. Eur. J.* **2002**, *8*, 2769−2774.
(11) (a) Bendele, G.; Stephens, P.; Prassides, K.; Vavekis, K.; Kortados, K.; Tanigaki, K. *Phys. Rev. Lett.* **1998**, *80*, 736−739. (b) Margadonna, S.; Prassides, K.; Knudsen, K.; Hanfland, M.; Kosaka, M.; Tanigaki, K. *Chem. Mater.* **1999**, *11*, 2960−2965.
(12) Broderick, W. E.; Choi, K. W.; Wan, W. C. *Electrochemical Soc. Proc.* **1997**, *14*, 1102−1113.
(13) Oszlányi, G.; Baumgarther, G.; Faigel, G.; Forró, L. *Phys. Rev. Lett.* **1997**, *78*, 4438−4441.


**10.1021/ja035546a CCC: $25.00** 

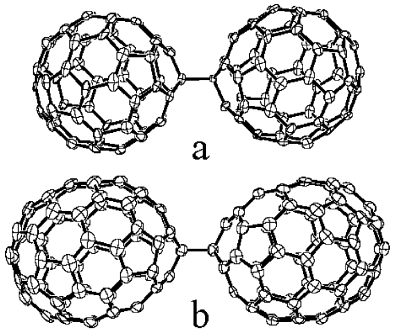


***Figure 1.*** Molecular structure of the $(C_{60}^-)_2$ dimer in $Cp^*_2Cr{\cdot}C_{60}{\cdot}(C_6H_4Cl_2)_2$ (**1**)[18](a); and the $(C_{70}^-)_2$ dimer in $CTV{\cdot}(Cs)_2{\cdot}(C_{70})_2{\cdot}(DMF)_7{\cdot}(C_6H_6)_{0.75}$ (**3**)[19] (b).

***Table 1.*** UV−vis−NIR Spectra of **1**−**10**

| solution | | | solid state in KBr pellets | | | |
|---|---|---|---|---|---|---|
| donor | bands, nm | attribution[a] | N | state at RT | UV | NIR range |
| $Cp^*_2Cr$ | 840, 941, 1313 ($CH_3CN$) | $C_{60}^{2-}$ | **1** | $C_{60}^{\bullet-}$ | −, 340 | 935, 1080 |
| | | | **2** | $C_{60}^{\bullet-}$ | −, 340 | 932, 1082 |
| | | | **3** | $(C_{70}^-)_2$ dimer | | 910, 1240 |
| $Cr(C_6H_6)_2$ | 941, 1073 ($CH_3CN$) | $C_{60}^{\bullet-}+C_{60}^{2-}$ | **4** | $C_{60}^{\bullet-}$ | 265, 341 | 936, 1078 |
| | | | **5** | $C_{60}^{\bullet-}$ | 267, 345 | 935, 1073 |
| | | | **6** | $(C_{70}^-)_2$ dimer | | 910, 1240 |
| | | | **7** | $(C_{60}^-)_2$ dimer or polymer | 261, 335 | 906, 1060, 1240 |
| $Cp_2Co$ | 827, 940 ($CH_3CN$) | $C_{60}^{2-}$ | **8** | $C_{60}^{\bullet-}$ | 266, 342 | 935, 1080 |
| | | | **9** | $(C_{70}^-)_2$ dimer | − | 910, 1240 |
| | | | **10** | $(C_{70}^-)_2$ dimer | − | 910, 1240 |
| $Cp_2Cr$ | 933, 1077 ($C_6H_5CN$) | $C_{60}^{\bullet-}$ | | | | |

[a] The characteristic absorption bands of $C_{60}^{\bullet-}$ in $C_6H_5CN$ are at 936−940 and 1080−1081 nm and those of $C_{60}^{2-}$ in $C_6H_5CN$ are at 840−844, 955−957, and 1321−1332 nm.[24]

attributed to the $C_{60}^{\bullet-}$ dimerization was observed in $Cr(C_6H_5Me)_2{\cdot}C_{60}$ at 250 K, whose crystal structure was investigated by X-ray powder diffraction.[16,17] Recently, single crystals of ionic $C_{60}$ complex: $Cp^*_2Cr{\cdot}C_{60}{\cdot}(C_6H_4Cl_2)_2$ have been prepared and the molecular structure of the $(C_{60}^-)_2$ dimer has been determined (Figure 1a).[18] The phase transition associated with the $C_{60}^{\bullet-}$ dimerization was observed at 220−200 K. Single-bonded $(C_{70}^-)_2$ dimers (Figure 1b) were found in $CTV{\cdot}(Cs)_2{\cdot}(C_{70})_2{\cdot}(DMF)_7{\cdot}(C_6H_6)_{0.75}$,[19] $Cr(C_6H_6)_2{\cdot}C_{70}{\cdot}C_6H_5Me$,[20] and $TDAE{\cdot}C_{70}{\cdot}C_6H_5Me$.[21] The formation of the $(C_{70}^-)_2$ dimers in the first

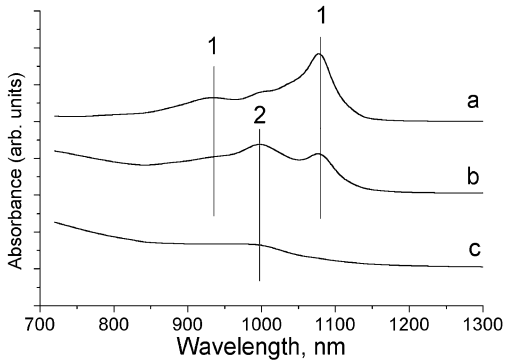


***Figure 2.*** Vis−NIR spectra of the benzonitrile solution containing $C_{60}$ and $Cp_2Cr$ at a 1:10 molar ratio: (a) 2 minutes after the preparation; (b) 1.5 hours after the preparation; (c) 3 hours after the preparation. Lines show the bands ascribable to $C_{60}^{\bullet-}$ (1) and zwitter-ion ($Cp_2Cr^+$-$C_{60}^{\bullet-}$) (2).

and the latter complexes was justified by the X-ray diffraction on a single crystal.[19,21] The study of these complexes seems promising due to that variation of donor and solvent molecules involved in the complex can lead to different dimers and polymers, whereas the possibility of the preparation of single crystals provides their structural characterization.

We systematically studied new ionic $C_{60}$ and $C_{70}$ complexes with strong donors, namely, decamethylchromocene ($Cp^*_2Cr$, $E^{+/0}_{1/2} = -1.04$ V[22]), bis(benzene)chromium ($Cr(C_6H_6)_2$, $E^{+/0}_{1/2} = -0.72$ V[23]), cobaltocene ($Cp_2Co$, $E^{+/0}_{1/2} = -0.91$ V[22]), chromocene ($Cp_2Cr$, $E^{+/0}_{1/2} = -0.55$ V[22]) (all $E^{+/0}_{1/2}$ vs. SCE), and cesium both in solution and solid state. The complexes were characterized by the elemental analysis, IR, UV−vis−NIR spectra, EPR, and SQUID measurements. The phase transitions attributed to the $C_{60}^{\bullet-}$ dimerization were found and the dimeric $(C_{60}^-)_2$ and $(C_{70}^-)_2$ phases were characterized. The IR and UV−vis−NIR spectra of $\sigma$-bonded negatively charged fullerenes have been presented. The reversibility of dimerization and the effect of the donor and solvent molecules involved in the complex on dimerization temperatures were studied.

## Results and Discussion

**Formation of Ionic Complexes.** The interaction of $C_{60}$ with donors was studied in solution. $C_{60}$ and a 10-fold molar excess of the donors were dissolved in benzonitrile ($C_6H_5CN$) or acetonitrile ($CH_3CN$) in anaerobic conditions. According to the NIR spectra, $C_{60}$ was reduced by $Cp_2Cr$ to $C_{60}^{\bullet-}$, $Cr^0(C_6H_6)_2$ to form the mixture of $C_{60}^{\bullet-}$ and $C_{60}^{2-}$, and $Cp^*_2Cr$ and $Cp_2Co$ to $C_{60}^{2-}$ (Table 1).[8a,24] The spectra of solutions remain unchanged during several hours (excepting $Cp_2Cr$) indicating the formation of stable ions.

Dissolution of $Cp_2Cr$ and $C_{60}$ produces initially violet solution in $C_6H_5CN$, which turns red-brown in 1.5 h and green-brown in 3 h. The NIR spectra (Figure 2) show the decay of characteristic absorption of $C_{60}^{\bullet-}$ at 933 and 1077 nm and the evolution of a new broad peak with the maximum at 1000 nm. The total intensity of absorption in the NIR range also decreases with time. Such a change is similar to that in the interaction of $C_{60}$ with unsaturated amines 1,8-diazabicyclo-[5,4,0]-undec-7-

(14) (a) Zhu, Q.; Cox, D. E.; Fischer, J. E. *Phys. Rev. B* **1995**, *51*, 3966−3969. (b) Oszlányi, G.; Bortel, G.; Faigel, G.; Tegze, M.; Grárásy, L.; Pekker, S.; Stephens, P. W.; Bendele, G.; Dinnebier, R.; Mihály, G.; Jánossy, A.; Chauvet, O.; Forró, L. *Phys. Rev. B* **1995**, *51*, 12 228−12 232. (c) Oszlányi, G.; Bortel, G.; Faigel, G.; Gránásy, L.; Bendele, G.; Stephens, P. W.; Forró, L. *Phys. Rev. B* **1996**, *54*, 11 849−11 852.; (d) Kosaka, M.; Tanigaki, K.; Tanaka, T.; Atake, T.; Lappas, A.; Prassides, T. *Phys. Rev. B* **1995**, *51*, 12 018−12 021.

(15) (a) Hummelen, J. C.; Khight, B.; Pavlovich, J.; Gonzales, R.; Wudl. F. *Science* **1995**, *269*, 1554−1556. (b) Simon, F.; D. Arčon, D.; Tagmatarchis, N.; Garaj, S.; Forro, L.; Prassides, K.; *J. Phys. Chem. A* **1999**, *103*, 6969−6971. (c) Hasharoni, K.; Bellavia-Lund, C.; Keshavarz-K, M.; Srdanov, G.; Wudl, F. *J. Am. Chem Soc*. **1997**, *119*, 11 128−11 129.

(16) Hönnerscheid, A.; Wüllen, L.; Jansen, M.; Rahmer, J.; Mehring, M. *J. Chem. Phys*. **2001**, *115*, 7161−7165.

(17) Hönnerscheid, A.; Dinnebier, R.; Jansen, M.; *Acta Crystallogr. Sect. B* **2002**, *58*, 482−488.

(18) Konarev, D. V.; Khasanov, S. S.; Otsuka, A.; Saito, G. *J. Am. Chem. Soc*. **2002**, *124*, 8520−8521.

(19) Konarev, D. V.; Khasanov, S. S.; Vorontsov, I. I.; Saito,G.; Antipin, Yu. M.; Otsuka, A.; Lyubovskaya, R. N. *Chem. Commun*. **2002**, 2548−2549.

(20) Yoshida, Y.; Otsuka, A.; Konarev, D. V.; Saito, G. *Synth. Met*. **2003**, *133*−*134*, 703−705.

(21) Oshima, K.; Kambe, T.; Fujiwara, M.; Nogami, Y. *Synth. Met*. **2003**, *133*−*134*, 609−701.

(22) Robbins, J. L.; Edelstein, N.; Spencer, B.; Smart, J. C. *J. Am. Chem. Soc*. **1982**, *104*, 1882−1893.

(23) Treichel, P. M.; Essenmacher, G. P.; Efner, H. F.; Klabunde, K. J. *Inorg. Chim. Acta* **1981**, *48*, 41−44.

(24) Konarev, D. V.; Drichko, N. V.; Graja, A. *J. Chim. Phys.* **1998**, *95*, 2143−2156.

***Table 2.*** Data for the Crystals of **1**−**10**

| N | complex | elemental analysis C,% | H,% | N,% | found/calcd. Cl,% | O,% | M, % | color and shape |
|---|---|---|---|---|---|---|---|---|
| **1** | $Cp^*_2Cr{\cdot}C_{60}{\cdot}(C_6H_4Cl_2)_2$ | according to X-ray diffraction data [18] | | | | | | black parallelepipeds |
| **2** | $Cp^*_2Cr{\cdot}C_{60}{\cdot}(C_6H_6)_2$ | 88.19 | 3.25 | 0.0 | | 8.56[a] | | black parallelepipeds |
| | | /89.77 | /3.41 | /0.0 | | /2.60 | /4.22 | |
| **3** | $CTV{\cdot}(Cs)_2{\cdot}(C_{70})_2{\cdot}(DMF)_7{\cdot}(C_6H_6)_{0.75}$ | according to X-ray diffraction data[19] | | | | | | black hexagonal plates |
| **4** | $Cr(C_6H_6)_2{\cdot}C_{60}{\cdot}(C_6H_4Cl_2)_{0.7}$ | 85.14 | 1.37 | | 4.67 | 8.82[a] | | black-brown polycrystals |
| | | /86.04 | /1.39 | | /4.67 | /3.01 | /4.89 | |
| **5** | $Cr(C_6H_6)_2{\cdot}C_{60}{\cdot}C_6H_5CN$ | 88.25 | 1.91 | 1.42 | 0.0 | 8.42[a] | | black parallelepipeds |
| | | /89.19 | /1.60 | /1.31 | /0.0 | /3.01 | /4.89 | |
| **6** | $Cr(C_6H_6)_2{\cdot}C_{70}{\cdot}C_6H_4Cl_2$ | 85.88 | 1.49 | | 4.76 | 7.87[a] | | black-brown |
| | | /86.08 | /1.30 | | /5.78 | /2.60 | /4.24 | polycrystals |
| **7** | $Cr(C_6H_6)_2{\cdot}C_{60}$ | 89.65 | 1.85 | | | 8.5[a] | | black-brown powder |
| | | /90.16 | /1.73 | | | /3.10 | /5.01 | |
| **8** | $Cp_2Co{\cdot}C_{60}{\cdot}C_6H_4Cl_2$ | 84.21 | 2.27 | | 5.70 | 7.82[a] | | black polycrystals |
| | | /83.84 | /1.28 | | /6.52 | /2.94 | /5.42 | |
| **9** | $Cp_2Co{\cdot}C_{70}{\cdot}(C_6H_4Cl_2)_{0.5}$ | 86.48 | 1.65 | 0.0 | 2.86 | 9.01[a] | | black polycrystals |
| | | /87.79 | /1.06 | /0.0 | /3.13 | /2.82 | /5.20 | |
| **10** | $Cs{\cdot}C_{70}{\cdot}(DMF)_5$ | 74.62 | 2.12 | 4.23 | | 19.09[a] | | elongated plates |
| | | /75.21 | /2.55 | /4.37 | | /8.17 | /9.70 | |

[a] Calculated by the difference (100,%) − ((C, H, Cl, N), %)

ene and 1,1′,3,3′-tetramethyl-$\Delta^{2,2'}$-bi(imidazoline) in $C_6H_5CN$.[25] In both cases, this interaction can be described by a two-step model. On the first fast step $C_{60}$ is reduced by chromocene to form individual $Cp_2Cr^+$ and $C_{60}^{\bullet-}$ ions. The second slow step is the addition of $Cp_2Cr^+$ to $C_{60}^{\bullet-}$ accompanied by the formation of covalently linked (probably by $\eta^2$-type) zwitter-ionic compound ($Cp_2Cr^+-C_{60}^{\bullet-}$) followed by radical recombination in this compound ($Cp_2Cr-C_{60}$). The reaction of $C_{60}$ with vanadocene,[26] titanocene,[27] and nickelocene[28] also yields the $(\eta^2\text{-}Cp_2M)_xC_{60}$ compounds.

The crystals of $C_{60}$ and $C_{70}$ complexes (Table 2) with $Cp^*_2Cr$, $Cr^0(C_6H_6)_2$, and $Cp_2Co$ were obtained by dissolution of fullerene and corresponding donor in $C_6H_4Cl_2$ (**1**, **4**, **6**, and **8**), $C_6H_6/C_6H_5CN$ (**2**, and **5**), $C_6H_4Cl_2/C_6H_5CN$ (**9**), and $C_6H_6$/DMF (**3**, **10**) mixtures and their crystallization during slow diffusion of hexane. Mixing $C_{60}$ and $Cr^0(C_6H_6)_2$ in $C_6H_6$ or $C_6H_5Me$ results in solid polycrystalline **7**.

**$C_{60}$ Complexes with Decamethylchromocene ($Cp^*_2Cr$).** $C_{60}$ forms $Cp^*_2Cr{\cdot}C_{60}{\cdot}(C_6H_4Cl_2)_2$ (**1**), and $Cp^*_2Cr{\cdot}C_{60}{\cdot}(C_6H_6)_2$ (**2**) depending on solvent used.

The IR and vis−NIR spectra of **1** and **2** are similar at room temperature (RT = 285 K) and show the ionic ground state of the complexes with monomeric $C_{60}^{\bullet-}$. It was justified by the shift of $F_{1u}(4)$ mode of $C_{60}$ in the complexes to 1392−1393 $cm^{-1}$ relative to $C_{60}$ (1429 $cm^{-1}$) and the essential increase of the integral intensities of $F_{1u}(2)$ (575 $cm^{-1}$) and $F_{1u}(4)$ modes relative to that of $F_{1u}(1)$ mode (526 (**1**) and 523 (**2**) $cm^{-1}$) as in $C_{60}^{\bullet-}$ radical anion salts $(Rb^+){\cdot}(C_{60}^{\bullet-})$[29] and $(Ph_4X^+)_2{\cdot}(C_{60}^{\bullet-}){\cdot}(Y^-)$ (X= P, As; Y= Cl, I).[30] The intense bands in the solid-state vis−NIR spectra of **1** and **2** (Table 1) also indicate the formation of $C_{60}^{\bullet-}$.[8a,24] The band of neutral $Cp^*_2Cr$ at 418 $cm^{-1}$ is shifted to 437 $cm^{-1}$ in **1**, to 438 $cm^{-1}$ in **2** and to 437 $cm^{-1}$ in ionic $(Cp^*_2Cr^+){\cdot}(PF_6^-)$,[22] indicating the formation of $Cp^*_2Cr^+$ in **1** and **2**. The absence of additional bands in the IR spectra, excepting solvent ones, which must appear at dimerization or polymerization of $C_{60}^{\bullet-}$[31] corresponds to the monomeric state of $C_{60}^{\bullet-}$.

The fragment of the RT crystal structure of **1**[18] is shown in Figure 3a. The complex contains orientationally disordered monomeric $C_{60}^{\bullet-}$ and ordered $Cp^*_2Cr^+$ (not depicted in Figure 3a). The $C_6H_4Cl_2$ molecules are disordered between two orientations linked to each other by rotation about the mass center in the molecular plane. Monomeric $C_{60}^{\bullet-}$ forms the zigzag chains along the diagonal to the *ac*-plane with the equal center-to-center distance of 10.10 Å (10.02 Å for pristine $C_{60}$ at RT[32]).

A reversible structural transformation accompanied by the unit cell multiplication takes place upon cooling **1** below 220−200 K. The zigzag chain arrangement of $C_{60}^-$ is observed in a low-temperature (100 K) dimeric structure as well (Figure 3b). However, the distances between the centers of $C_{60}^-$ are not equal: one short distance of 9.28 Å indicates the formation of a $\sigma$-bonded $(C_{60}^-)_2$ dimer and the second distance of 9.91 Å is close to that in the RT structure of **1** and pristine $C_{60}$ at 153 K (9.94 Å[33]).

The $(C_{60}^-)_2$ dimers are statistically disordered between two orientations linked to each other by rotation of $(C_{60}^-)_2$ about the intercage C−C bond by an angle of 142°. The occupancy factors are 0.75 and 0.25. The length of intercage C−C bond in the $(C_{60}^-)_2$ dimer is 1.597(7) Å. The estimated intercage C−C bond dissociation energy is 63 ± 4[18] and 35 ± 5 kJ·$mol^{-1}$ for **1** and **2**, respectively.

Magnetic susceptibilities of **1** and **2** were measured in the 300−1.9 K range (Table 3). The temperature dependencies of their magnetic moments ($\mu_{eff}$) are presented in Figure 4. The

(25) (a) Skiebe, A.; Hirsch, A.; Klos, H.; Gotschy, B. *Chem. Phys. Lett.* **1994**, *220*, 138−140. (b) Schilder, A.; Gotschy, B.; Seidl, A.; Gompper, R. *Chem. Phys.* **1995**, *193*, 321−326.
(26) Cherkasov, V. K.; Rad'kov, Yu. F.; Lopatin, M. A.; Bochkarev, M. N. *Russ. Chem. Bull.* **1994**, *43*, 1834−1836.
(27) Burlakov, V. V.; Usatov, A. V.; Lyssenko, K. A.; Antipin, M. Yu.; Novikov, Yu. N.; Shur, V. B. *Eur. J. Inorg. Chem.* **1999**, 1855−1857.
(28) Konarev, D. V.; Lyubovskaya, R. N.; Drichko, N. V.; Yudanova, E. I.; Shul'ga, Yu. M.; Litvinov, A. L.; Semkin, V. N.; Tarasov, B. P. *J. Mater. Chem.* **2000**, 803−818.
(29) Picher, T.; Winkler, R.; Kuzmany, H. *Phys. Rev. B, Solid State* **1994**, *49*, 15 879−15 889.
(30) Semkin, V. N.; Spitsina, N. G.; Krol, S.; Graja, A. *Chem. Phys. Lett.* **1996**, *256*, 616−622.
(31) Dresselhaus, M. S.; Dresselhaus, G. In *Fullerene Polymers and Fullerene Polymer Composites*; Eklund, P. C., Rao, A. M., Eds.; Springer-Verlag: Berlin, 1999, p 1−57.
(32) Heiney, P. A.; Fischer, J. E.; McGhie, A. R.; Romanov, W. J.; Denenstein, A. M.; McCauley, J. P., Jr.; Smith, A. B., III; Cox, D. E. *Phys. Rev. Lett.* **1991**, *67*, 1468−1468.
(33) Burgi, H.-B.; Blanc, E.; Schwarzenbach, D.; Liu, S.; Lu, Y.-J.; Kappers, M. M.; Ibers, J. A. *Angew. Chem., Int. Ed. Engl.* **1992**, *31*, 640−643.

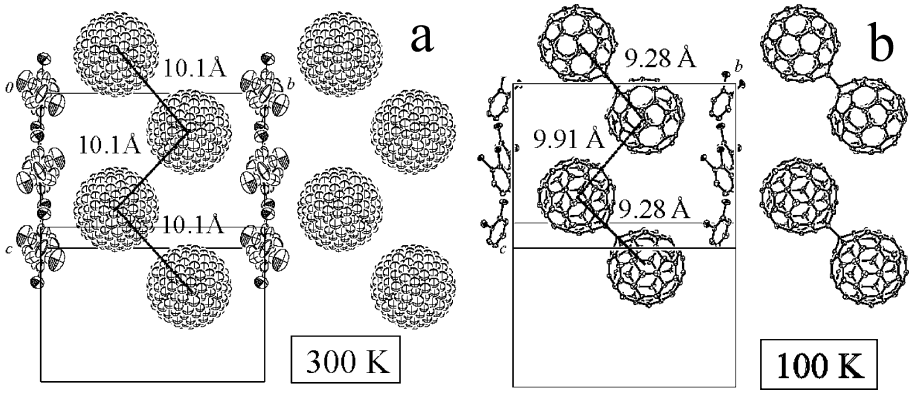


***Figure 3.*** Packing of $C_{60}^-$ and $C_6H_4Cl_2$ in $Cp^*_2Cr{\cdot}C_{60}{\cdot}(C_6H_4Cl_2)_2$ (**1**) at 300 (a) and 100 K (b). $Cp^*_2Cr^+$ cations are omitted for clarity. The view along the diagonal to the *ac*-plane is shown. Zigzag chains from $C_{60}^-$ are shown by dashed lines. Only the major orientation of the $(C_{60}^-)_2$ dimers is shown for low temperature structure (b).

***Table 3.*** Data of Magnetic Measurements

| N | Θ, K (temp range, K) | observed $\mu_{eff}$,$\mu_B$ (temp. range, K) | calculated $\mu_{eff}$,$\mu_B$ per formula unit |
|---|---|---|---|
| **1** | −1.12 (50−190) | 3.85 (50−190) | 3.87 ($S$ = 3/2) |
| | | 4.20 (240−300) | 4.27 ($S$ = 3/2, 1/2) |
| **2** | −0.85 (10−160) | 3.80 (10−160) | 3.87 ($S$ = 3/2) |
| | | 4.14 (190−300) | 4.27 ($S$ = 3/2, 1/2) |
| **3** | −0.51 (2−350) | | Complex is diamagnetic ($\chi_0$= −0.0017 emu·mol$^{-1}$). The Curie tail corresponds to 2.4% of total $C_{70}$ |
| **4** | −0.06 (10−140) | 1.73 (10−160) | 1.73 ($S$ = 1/2) |
| | | 2.40−2.45 (240−300) | 2.45 ($S$ = 1/2, 1/2) |
| **5** | −0.18 (10−220) | 1.74 (10−220) | 1.73 ($S$ = 1/2) |
| | | 2.12 (300) | 2.12 (intermediate value between $S$ = 1/2 and $S$ = 1/2, 1/2) |
| **6** | −0.06 (10−250) | 1.64 (10−250) | 1.73 ($S$ = 1/2) |
| | | 1.78 (300) | |
| **7** | −3.5 (70−300) | 1.80 (70−300) | 1.73 ($S$ = 1/2) |
| **8** | −0.72 (2−250) | 0.04−0.08 (1.9−250) | Complex is diamagnetic. The Curie tail corresponds to 3.3% of total $C_{60}$ |
| | | 1.52 (350−380) | 1.73 ($S$=1/2) |
| **10** | −0.46 (2−350) | | Complex is diamagnetic ($\chi_0$ = −0.0025 emu·mol$^{-1}$). The Curie tail corresponds to 0.7% of total $C_{70}$ |

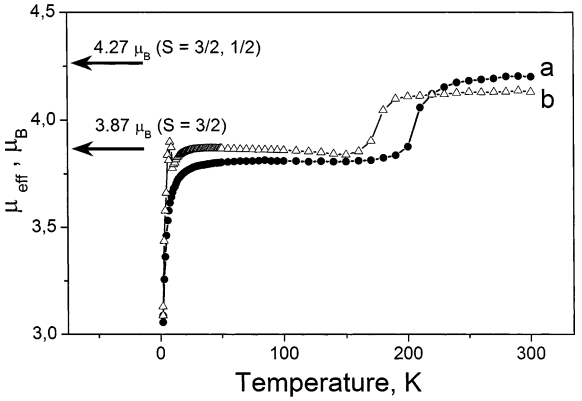


***Figure 4.*** Dependencies of the magnetic moment ($\mu_{eff}$) *vs* temperature for polycrystalline (a) $Cp^*_2Cr{\cdot}C_{60}{\cdot}(C_6H_4Cl_2)_2$ (**1**), and (b) $Cp^*_2Cr{\cdot}(C_{60}){\cdot}(C_6H_6)_2$ (**2**) between 300 and 1.9 K. The behavior is reversible.

magnetic moments are equal to 4.14−4.20 $\mu_B$ at 300 K (the $\mu_{eff}$ for the noninteracting $S$ = 3/2, 1/2 system is 4.27 $\mu_B$). Therefore, both spins from $Cp^*_2Cr^+$ ($S$ = 3/2) and $C_{60}^{\bullet-}$ ($S$ = 1/2) contribute to magnetic susceptibility. A close value of 4.20 $\mu_B$ was observed in $(Cr^{III}TPP^+){\cdot}(C_{60}^{\bullet-}){\cdot}(THF)_3$[7] with the same spin state ($S$ = 3/2, 1/2). A stepwise reversible decrease in the magnetic moment of **1** and **2** from 4.14 to 4.20 down to 3.81−3.88 $\mu_B$ was detected in the 230−200 K and 190−160 K ranges for **1** and **2**, respectively (Figure 4). Below these temperatures the magnetic moments are defined by the spins localized on $Cp^*_2Cr^+$ (the $\mu_{eff}$ for the $S$ = 3/2 system is 3.87 $\mu_B$). The decrease in the magnetic moment of **1** and **2** clearly indicates the disappearance of the contribution of $C_{60}^{\bullet-}$ spins ($S$ = 1/2) consistent with the reversible formation of the diamagnetic $(C_{60}^-)_2$ dimers. The reversible decrease of the magnetic moment from 2.5 $\mu_B$ down to 1.72 $\mu_B$ was also observed in $Cr(C_6H_5Me)_2{\cdot}C_{60}$ at 250 K as a result of $C_{60}^{\bullet-}$ dimerization.[16] The decrease in the magnetic moments of **1** and **2** below 30 K (Figure 4) indicates a weak antiferromagnetic interaction between the $Cp^*_2Cr^+$ spins. However, the spin ordering was not observed down to 1.9 K.

The EPR signals for **1** and **2** were not observed at RT (Figure 5 shows the EPR spectrum of **1** at 250 K). Similarly, ionic $Cr^{III}TPP{\cdot}C_{60}{\cdot}(THF)_3$ is EPR silent in the 300−4 K range.[7] It can be assumed that monomeric $C_{60}^{\bullet-}$ and $Cp^*_2Cr^+$ can give one very broad resonating signal via a strong exchange coupling between these ions. Upon cooling **1** below 220−200 K (Figure 5, 200 and 4 K) and **2** below 180−160 K, new signals appear in the EPR spectra. The signal in **1** is asymmetric and is characterized by resonances near $g_\perp$=3.974 with the line half-width ($\Delta H$) of 7 mT and $g_\parallel$ = 2.013 with $\Delta H$ = 5.5 mT at 4 K. This signal can be ascribed to $Cp^*_2Cr^+$ with $S$ = 3/2 ground state. Solid $(Cp^*_2Cr^+)(PF_6^-)$[22] produces a similar EPR signal with $g_\perp$ = 4.02(1) and $g_\parallel$ = 2.001(1). The g-factor and $\Delta H$ of

***Table 4.*** EPR Parameters (g-factor and the line half-width ($\Delta H$)) for **1**−**10** at RT (285 K) and 4 K

| N | RT | | attribution of the signal | 4 K | | attribution of the signal |
|---|---|---|---|---|---|---|
| | g-factor | $\Delta H$, mT | | g-factor | $\Delta H$, mT | |
| **1** | not observed | | | 3.974 | 7.0 | $Cp^*_2Cr^+$ (S=3/2), $g_\perp$ |
| | | | | 3.728 | 12.3 | |
| | | | | 3.467 | 14.0 | |
| | | | | 2.013 | 5.5 | $g_{II}$ |
| **2** | not observed | | | 3.937 | 7.7 | $Cp^*_2Cr^+$ (S=3/2), $\perp$ |
| | | | | 3.784 | 17.0 | |
| | | | | 3.417 | 18.8 | |
| **3** | 2.0042 | 0.8 | impurity (<0.4% | | | |
| | 2.0024 | 0.2 | of total $C_{70}$) | | | |
| | 1.9923 | 2.0 | | | | |
| **4** | 1.9913 | 3.30 | $Cr^I(C_6H_6)_2^{\bullet+} + C_{60}^{\bullet-}$ | 1.9858 | 2.21 | $Cr^I(C_6H_6)_2^{\bullet+}$ |
| **5** | 1.9910 | 2.94 | $Cr^I(C_6H_6)_2^{\bullet+} + C_{60}^{\bullet-}$ | 1.9949 | 2.78 | $Cr^I(C_6H_6)_2^{\bullet+}$, $g_{II}$ |
| | | | | 1.9835 | 2.46 | $g_\perp$ |
| **6** | 1.9857 | 3.10 | $Cr^I(C_6H_6)_2^{\bullet+}$ | 1.9859 | 2.75 | $Cr^I(C_6H_6)_2^{\bullet+}$ |
| **7** | 1.9977 | 1.71 | $Cr^I(C_6H_6)_2^{\bullet+}$, $g_{II}$ | 1.9957 | 2.02 | $Cr^I(C_6H_6)_2^{\bullet+}$, $g_{II}$ |
| | 1.9901 | 1.74 | $g_\perp$ | 1.9858 | 1.74 | $g_\perp$ |
| **8** | 1.9988 | 3.97 | $C_{60}^{\bullet-}$ | 1.9979 | 0.5 | $C_{60}^{\bullet-}$ (calc.2−3% ot total |
| | | | | 1.9998 | 0.3 | $C_{60}$ |
| **9** | 2.0025 | 0.26 | impurities (<0.1% ot total | 2.0047 | 0.76 | trace of $C_{70}^{\bullet-}$ |
| | 2.0013 | 0.15 | $C_{70}$) | 2.0027 | 0.36 | impurity |
| **10** | 2.0025 | 0.22 | impurity (<1% of total $C_{70}$) | 2.0025 | 0.15 | impurity |

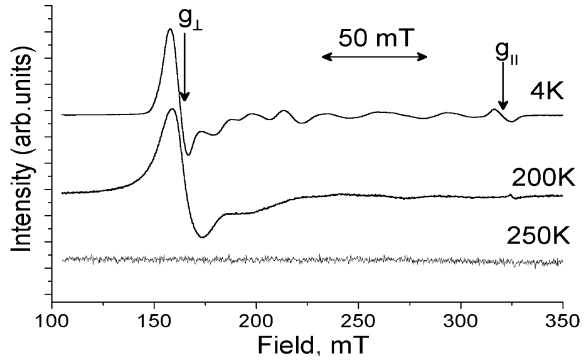


***Figure 5.*** EPR spectrum of polycrystalline $Cp^*_2Cr{\cdot}C_{60}{\cdot}(C_6H_4Cl_2)_2$ (**1**) at 4200 and 250 K.

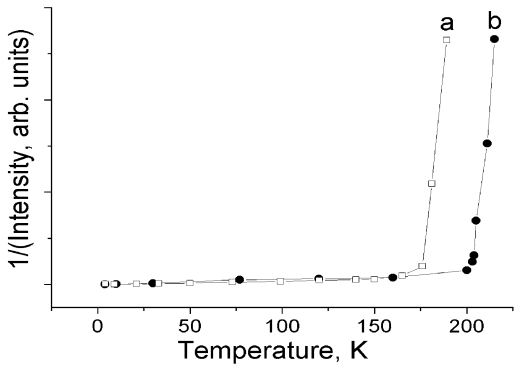


***Figure 6.*** Temperature dependencies of reversible intensity of the EPR signal from $Cp^*_2Cr^+$ ($S = 3/2$) in polycrystalline (a) $Cp^*_2Cr{\cdot}(C_{60}){\cdot}(C_6H_6)_2$ (**2**) and (b) $Cp^*_2Cr{\cdot}C_{60}{\cdot}(C_6H_4Cl_2)_2$ (**1**).

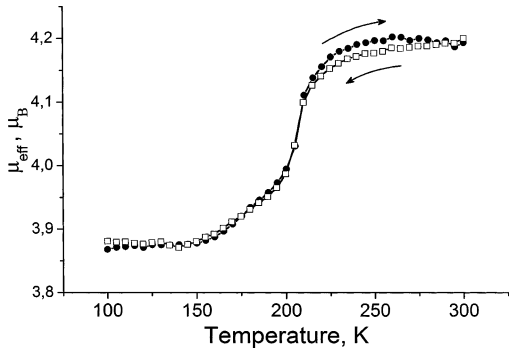


***Figure 7.*** Temperature dependency of magnetic moment ($\mu_{eff}$) for polycrystalline $Cp^*_2Cr{\cdot}C_{60}{\cdot}(C_6H_4Cl_2)_2$ (**1**) upon the heating (full circles) and cooling (open squares) processes.

the EPR signal from $Cp^*_2Cr^+$ in **1** and **2** only weakly depend on temperature down to 4 K. The $g_\perp$-component of the EPR signal of polycrystalline **1** is strongly asymmetric and consists of at least 9 components. The most intense component has $g_1 = 3.974$ and $\Delta H = 7$ mT and each next component shifts to smaller *g*-factor and becomes wider (Table 4). For **2** the spectrum is similar. The asymmetric EPR signals in **1** and **2** are probably a result of polycrystallinity of the samples.

The temperatures of the appearance of the EPR signals from $Cp^*_2Cr^+$ in **1** and **2** (Figure 6) correlate with those of the disappearance of the contribution of the $C_{60}^{\bullet-}$ spins to magnetic susceptibility (Figure 4). The formation of the diamagnetic $(C_{60}^-)_2$ dimer breaks down the exchange coupling between $Cp^*_2Cr^+$ and monomeric $C_{60}^{\bullet-}$ at RT and leads to EPR active species containing paramagnetic $Cp^*_2Cr^+$ and the diamagnetic $(C_{60}^-)_2$ dimers at low temperatures.

The temperature dependency of magnetic susceptibility of polycrystalline **1** in the cooling and heating processes was studied in the 100−300 K range (Figure 7). At a slow rate (5 K per minute, the waiting time is 3 h at 100 and 300 K) the temperature dependency of magnetic moment of **1** is nearly the same for both processes with the hysteresis smaller than 2 K.

**Complex of $C_{70}$ Fulleride with Cyclotriveratrylene (CTV).** According to the X-ray diffraction on a single crystal the multicomponent complex $CTV{\cdot}(Cs)_2{\cdot}(C_{70})_2{\cdot}(DMF)_7{\cdot}(C_6H_6)_{0.75}$ (**3**) contains single-bonded $(C_{70}^-)_2$ dimers, which begin to dissociate above 300 K, and the abrupt increase in the magnetic moment is observed only above 360 K. The length of theintercage C−C bond in the $(C_{70}^-)_2$ dimer was found to be 1.584(9) Å.[19]

The IR and UV−vis−NIR spectra of **3** indicate an essential spectral difference between the $(C_{70}^-)_2$ dimers and the monomeric $C_{70}^{\bullet-}$ radical anions (Figure 8). The solid NIR spectrum of $(C_{70}^-)_2$ is specified by the presence of two bands at 910 and 1240 nm (Figure 8b) instead of one band at 1373 nm in the

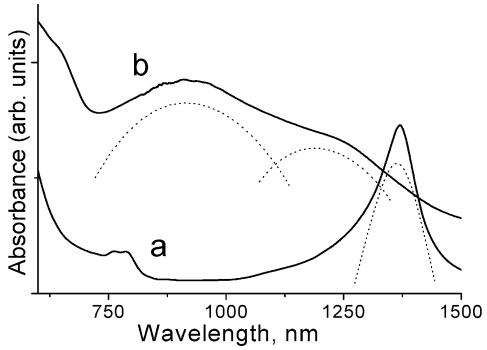


***Figure 8.*** Vis−NIR spectra of (a) monomeric $C_{70}^{\bullet-}$ generated in the $C_6H_4Cl_2$ solution by the reduction of $C_{70}$ with an equimolar amount of $Cr(C_6H_6)_2$; and (b) the $(C_{70}^-)_2$ dimer in polycrystalline CTV·$(Cs)_2$·$(C_{70})_2$·$(DMF)_7$·$(C_6H_6)_{0.75}$ (**3**) in KBr pellet.

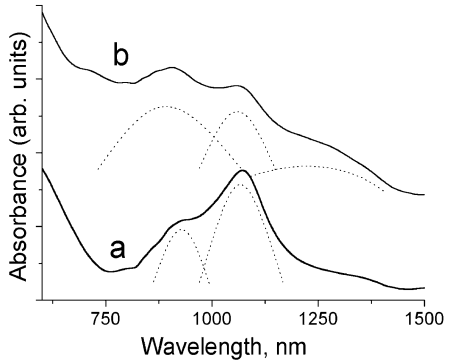


***Figure 9.*** Vis−NIR spectra of (a) monomeric $C_{60}^{\bullet-}$ in polycrystalline $Cr(C_6H_6)_2$·$C_{60}$·$(C_6H_4Cl_2)_{0.7}$ (**4**); and (b) the $(C_{60}^-)_2$ dimer or polymer in polycrystalline $Cr(C_6H_6)_2$·$C_{60}$ (**7**) in KBr pellets.

solution spectrum of $C_{70}^{\bullet-}$ (Figure 8a). The IR spectrum of $(C_{70}^-)_2$ consists of more than 20 bands,[19] whereas only 10 bands are pronounced in the spectrum of parent $C_{70}$. The appearance of additional "silent" modes is attributed to $C_{70}^-$ symmetry breaking in the dimer. These modes can be used to identify the $(C_{70}^-)_2$ dimers in the complexes.

**$C_{60}$ and $C_{70}$ Complexes with Bis(benzene)chromium ($Cr(C_6H_6)_2$).** Bis(benzene)chromium complexes of $C_{60}$ and $C_{70}$: $Cr(C_6H_6)_2$·$C_{60}$·$(C_6H_4Cl_2)_{0.7}$ (**4**), $Cr(C_6H_6)_2$·$C_{60}$·$C_6H_5CN$ (**5**), $Cr(C_6H_6)_2$·$C_{70}$·$C_6H_4Cl_2$ (**6**), and $Cr(C_6H_6)_2$·$C_{60}$ (**7**) have been obtained. According to the IR spectra, **4** and **5** also have the ionic ground state with monomeric $C_{60}^{\bullet-}$. $F_{1u}(4)$ $C_{60}$ mode shifts in the complexes to 1388−1390 $cm^{-1}$ whereas the bands of neutral $Cr^0(C_6H_6)_2$ at 459 and 490 $cm^{-1}$ shift to 418−419 and 460 $cm^{-1}$ in **4** and **5** as in $(Cr^I(C_6H_6)_2^{\bullet+})(I^-)$.[34] The solid NIR spectra of **4** and **5** contain the bands attributable to $C_{60}^{\bullet-}$ (Table 1, Figure 9 a).

The SQUID and EPR data for **4** and **5** are listed in Tables 3 and 4. The magnetic moment of **4** at RT (2.45 $\mu_B$) is close to calculated one for the $S = 1/2, 1/2$ system. These spins are localized on $Cr^I(C_6H_6)_2^{\bullet+}$ and $C_{60}^{\bullet-}$. The magnetic moment stepwise and reversibly decreases below 240 K down to 1.73 $\mu_B$ at 160 K (Figure 10, **4**) ($\mu_{eff}$ for $S = 1/2$ system is 1.73 $\mu_B$). This decrease is accompanied by the changes in the EPR spectrum. The EPR signal of **4** has $g = 1.9913$ at RT (Figure 11, **4**). This value is intermediate between those for $Cr^I(C_6H_6)_2^{\bullet+}$ ($g = 1.986$[35]) and $C_{60}^{\bullet-}$ ($g = 1.998$[8a]) indicating strong exchange coupling between these ions. On cooling **4** in the 240−150 K range the g-factor shifts to 1.986, that is characteristic of $Cr^I(C_6H_6)_2^{\bullet+}$ [35] (Figure 11, **4**).

The magnetic moment of **5** is 1.74 $\mu_B$ below 230 K and remains unchanged down to 10 K. Above 230 K the magnetic moment increases with temperature up to 2.12 $\mu_B$ at 300 K (the $\mu_{eff}$ intermediate between 1.73 $\mu_B$ ($S = 1/2$) and 2.45 $\mu_B$ ($S = 1/2, 1/2$)) (Figure 10, **5**). Probably, the magnetic moment can further increase with temperature up to ~2.45 $\mu_B$ above 350 K.

The EPR behavior of **5** is more complicated than that of **4** (Table 4, Figure 11, **5**). The EPR signal is a Lorentzian line with $g = 1.9910$ and $\Delta H = 3$ mT at RT. The g-factor shifts to 1.988 and the signal becomes narrower as in **4** with the temperature decrease down to 230 K. However, below 230 K, the signal broadens and splits into two components below 150 K ($g_{||} = 1.9949$ and $g_\perp = 1.9835$ at 4 K). Such asymmetric signal with $g_{||} = 2.0026$ and $g_\perp$=1.9757 was observed for $Cr^I(C_6H_6)_2^{\bullet+}$ in rigid solution.[35] The reason for the different symmetric and asymmetric EPR signals from $Cr^I(C_6H_6)_2^{\bullet+}$ in **4** and **5** is not clear. However, both SQUID and EPR measurements indicate a reversible disappearance of the contribution of the $C_{60}^{\bullet-}$ spins on cooling **4** and **5** in the 240−160 and 300−230 K ranges as a result of $C_{60}^{\bullet-}$ dimerization. The intercage C−C bond dissociation energy was estimated from the data of magnetic measurements to be 25 ± 2 and 41 ± 3 kJ·$mol^{-1}$ for **4** and **5**, respectively.

It was shown that in the spectrum of $Cr(C_6H_6)_2$·$C_{70}$·$C_6H_4Cl_2$ (**6**) the IR bands of $C_{70}$ appeared at same position[36a] as those in the spectrum of **3**[19] containing the $(C_{70}^-)_2$ dimers, whereas the IR bands at 418 and 459 $cm^{-1}$ indicated the presence of $Cr^I(C_6H_6)_2^{\bullet+}$. The two characteristic bands at 910 and 1240 nm in the NIR spectrum of **6** (as in Figure 8b) also justify the formation of $(C_{70}^-)_2$.

The magnetic moment of **6** is equal to 1.64 $\mu_B$ at 250 K and only slightly increases with temperature up to 1.78 $\mu_B$ at 300 K (Figure 10, **6**). The EPR signal of **6** with $g = 1.9857$ (Table 4) at RT is characteristic of $Cr^I(C_6H_6)_2^{\bullet+}$ [35] and does not shift with the temperature decrease down to 10 K (Figure 11, **6**). Such a behavior indicates the formation of the $(C_{70}^-)_2$ dimers and the contribution of only $Cr^I(C_6H_6)_2^{\bullet+}$ spins to magnetic and spin susceptibility**.** The increase of the magnetic moment of **6** above 250 K suggests the dissociation of the $(C_{70}^-)_2$ dimers to $C_{70}^{\bullet-}$ (about 8% of total $C_{70}$ at 300 K).

Fast precipitation of the complex in $C_6H_6$ or $C_6H_5Me$ yields solvent-free $Cr(C_6H_6)_2$·$C_{60}$ (**7**).[12,37] The IR spectrum of **7** is very rich at RT indicating the splitting of four $C_{60}$ modes into three components and the appearance of new weak "silent" modes.[36b] This spectrum differs from those of **4** and **5** and indicates broken symmetry of $C_{60}^-$ due to the formation of a $\sigma$-bonded structure. The formation of linear polymers in $(Rb^+)(C_{60}^{\bullet-})$ results in similar changes.[38] Instead of characteristic bands of $C_{60}^{\bullet-}$ new

(34) Fritz, H. P.; Lüttke, W.; Stammreich, H.; Forneris, R. *Chem. Ber*. **1959**, *92*, 3246−3250.

(35) Elschenbroich, C.; Bilger, E.; Koch, J. *J. Am. Chem. Soc.* **1984**, *106*, 4297−4299.

(36) (a) The absorption bands in IR-spectrum of **6** attributed to the $(C_{70}^-)_2$ dimer: 494w, 508w, 530s, 548m, 556m, 575m, 628w, 638w, 658w, 668w, 695w, 800s, 713w, 720m, 842m, 901w, 944w, 1110w, 1158m, 1176m, 1209w, 1258w, 1279m, 1307w, 1323m, 1353w, 1363w, 1392s, 1429m, 1415w, 1480w, 1508w, 1540w, 1558m $cm^{-1}$. (b) The absorption bands in IR-spectrum of **7** attributed to the $(C_{60}^-)_2$ dimer or polymer: 499w, 520w, 528w, 540s, 554w, 572s, 607s, 724m, 752w, 774s, 920w, 1010w, 1031w, 1121w, 1172w, 1194m, 1250w, 1322w, 1339w, 1383s, 1406m $cm^{-1}$.

(37) (a) Kaplunov, M. G.; Golubev, E. V.; Kulikov, A. V.; Spitsina, N. G. *Izv. Acad. Nauk, Ser. Khim.* 1999, 785−787. (b) Yoshida, Y.; Otsuka, A.; Drozdova, O. O.; Saito, G. *J. Mater. Chem.* **2003**, *13*, 252−257.

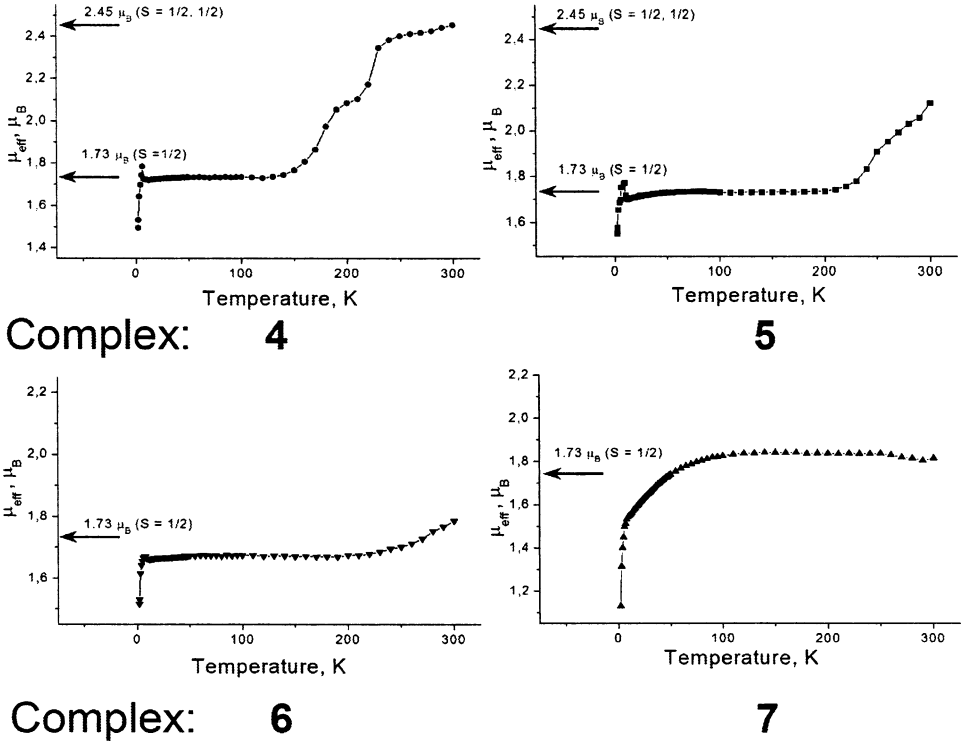


***Figure 10.*** Dependencies of the magnetic moment ($\mu_{eff}$) *vs* temperature for polycrystalline $Cr(C_6H_6)_2{\cdot}C_{60}{\cdot}(C_6H_4Cl_2)_{0.7}$ (**4**); $Cr(C_6H_6)_2{\cdot}C_{60}{\cdot}C_6H_5CN$ (**5**); $Cr(C_6H_6)_2{\cdot}C_{70}{\cdot}C_6H_4Cl_2$ (**6**); and $Cr(C_6H_6)_2{\cdot}C_{60}$ (**7**) between 300 and 1.9 K.

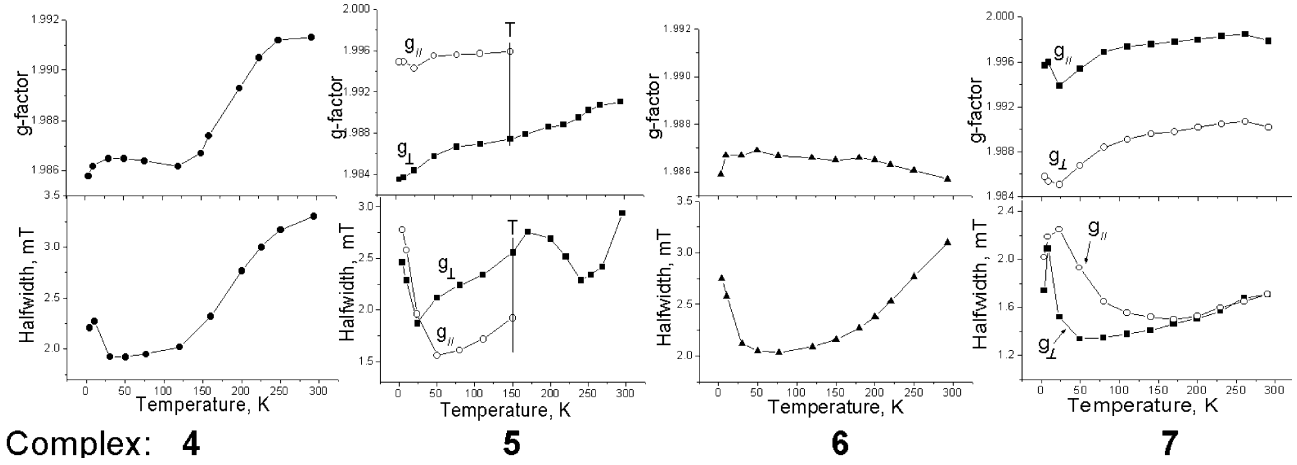


***Figure 11.*** Temperature dependencies of g-factor and the line half-width ($\Delta H$, mT) of the EPR signals from polycrystalline: $Cr(C_6H_6)_2{\cdot}C_{60}{\cdot}(C_6H_4Cl_2)_{0.7}$ (**4**); $Cr(C_6H_6)_2{\cdot}C_{60}{\cdot}C_6H_5CN$ (**5**); $Cr(C_6H_6)_2{\cdot}C_{70}{\cdot}C_6H_4Cl_2$ (**6**); and $Cr(C_6H_6)_2{\cdot}C_{60}$ (**7**).

bands appear in the NIR spectrum of **7** at 906, 1060, and 1240 nm (Figure 9b). These bands have not been found in the NIR spectra of **4** and **5** containing the same ions and can be attributed to the $\sigma$-bonded structure from $C_{60}^-$.

The magnetic moment of **7** is equal to 1.84 $\mu_B$ at 300 K and remains unchanged down to 70 K (Figure 10, **7**) indicating the contribution of one $S = 1/2$ spin. The EPR signal from **7** is asymmetric at RT and has two Lorentzian lines with $g_1 = 1.9979$ and $g_2 = 1.9902$ (Figure 11, **7**) similarly to the data of Broderick et al.[12] These lines can be attributed to the parallel and perpendicular components of the asymmetric signal from $Cr^I(C_6H_6)_2^{\bullet+}$ (Table 4). The splitting of the EPR signal in **7** is similar to that in **4** below 150 K. The EPR signal of $C_{60}^-$ has not been found and, hence, the spins are localized mainly on $Cr^I(C_6H_6)_2^{\bullet+}$. That is evidence of the formation of the $(C_{60}^-)_2$ dimers. However, the dimer in **7** is stable up to 300 K in contrast to dimers in other complexes studied. Therefore, another $\sigma$-bonded nondimeric structure composed of $C_{60}^-$ is also possibly formed. X-ray diffraction data are necessary for the precise determination of this structure.

The magnetic moments of the complexes decrease below 10 K for **4**−**6** and 70 K for **7** (Figure 10). The EPR signals from **4**−**7** noticeably broaden below these temperatures (Figure 11) indicating an antiferromagnetic interaction of the $Cr^I(C_6H_6)_2^{\bullet+}$ spins. The spin ordering is not observed down to 1.9 K.

**$C_{60}$ and $C_{70}$ Complexes with Cobaltocene ($Cp_2Co$).** Ionic $C_{60}$ complexes: $Cp_2Co{\cdot}C_{60}{\cdot}CS_2$,[4] $Cp_2Co{\cdot}C_{60}{\cdot}C_6H_5CN$[5], and $C_{70}$ complex: $Cp_2Co{\sim}C_{70}$[39] with cobaltocene were characterized,

(38) Kuzmany, H.; Winkler, R.; Pichler, T. *J. Phys. Condens. Matter* **1995**, 7, 6601−6624.

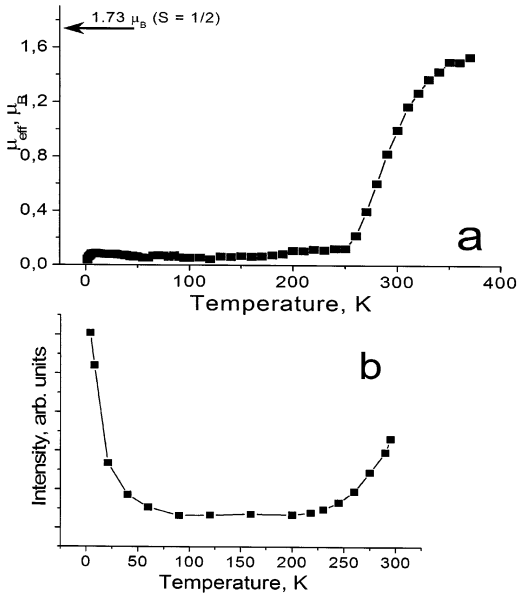


***Figure 12.*** Temperature dependencies of (a) the magnetic moment ($\mu_{eff}$) of $Cp_2Co{\cdot}C_{60}{\cdot}C_6H_4Cl_2$ (**8**) in the 1.9−380 K range; and (b) the intensity of the EPR signal from $C_{60}^{\bullet-}$ in **8** in the 4−285 K range.

and it is shown that they contain monomeric $C_{60}^{\bullet-}$ (at 123 K)[4] and $C_{70}^{\bullet-}$ (at 4−300 K).[39] We prepared new $C_{60}$ and $C_{70}$ complexes with cobaltocene $Cp_2Co{\cdot}C_{60}{\cdot}C_6H_4Cl_2$ (**8**), and $Cp_2Co{\cdot}C_{70}{\cdot}(C_6H_4Cl_2)_{0.5}$ (**9**), whose electronic states are different from those of the above-mentioned complexes.

The ionic ground state of **8** with monomeric $C_{60}^{\bullet-}$ at RT is justified by the characteristic bands in IR- and vis-NIR spectra (Table 1). However, the complex is a diamagnetic one in the 1.9−250 K range according to SQUID measurements and contains the diamagnetic $Cp_2Co^+$ cations and the $(C_{60}^-)_2$ dimers. The Curie tail in this temperature range corresponds to the contribution of only 3.3% of $S = 1/2$ spins. On heating **8** in the 250−350 K range, the reversible increase in the magnetic moment up to 1.52 $\mu_B$ (at 350 K) is observed (Figure 12 *a*) as a result of the dissociation of the $(C_{60}^-)_2$ dimers to $C_{60}^{\bullet-}$. Above 350 K, $C_{60}^-$ exists mainly in a monomeric form. The estimated intercage C−C bond dissociation energy is 52 ± 3 kJ mol$^{-1}$.

Two low-temperature signals were observed in the EPR spectrum of **8**. The main signal with $g = 1.9979$ and $\Delta H = 0.5$ (4 K) mT can be ascribed to $C_{60}^{\bullet-}$. The signal has weak intensity (calc. only 2−3% from the total amount of $C_{60}$) and the major part of the complex is EPR silent. The paramagnetic contribution (the Curie tail) to magnetic and spin susceptibility of **8** in the 1.9−250 K range is given by only 2−3% of spins localized on $C_{60}^{\bullet-}$. These spins are preserved in the sample probably due to incomplete $C_{60}^{\bullet-}$ dimerization at high enough cooling rate. Above 250 K, the intensity of the EPR signal of $C_{60}^{\bullet-}$ increases (Figure 12, *b*) in accordance with the magnetic measurements. A narrow weak signal with $g = 1.9998$ and $\Delta H$ of 0.3 mT (4 K) attributed to reduced impurities[40] has an almost temperature independent g-factor and $\Delta H$ in the 4−285 K range.

The IR and solid-state NIR (Table 1) spectra of $Cp_2Co{\cdot}C_{70}{\cdot}(C_6H_4Cl_2)_{0.5}$ (**9**) contain bands characteristic of the $(C_{70}^-)_2$ dimer. Two bands of the $(C_{70}^-)_2$ dimer at 910 and 1240 nm are clearly distinguished from single band at 1373 nm in the solid-state spectrum of related $Cp_2Co{\sim}C_{70}$[39] with monomeric $C_{70}^{\bullet-}$. **9** is EPR silent and shows only a weak EPR signal (<0.1% of total $C_{70}$) in the 4−285 K range attributable to impurities.[40] Thus, **9** is formulated as $(Cp_2Co^+)_2{\cdot}[(C_{70}^-)_2]{\cdot}(C_6H_4Cl_2)$ below 285 K.

**$C_{70}$ Complex with Cs.** The complex crystallizes from DMF as $Cs{\cdot}C_{70}{\cdot}(DMF)_5$ (**10**). The IR and NIR (Table 1) spectra of **10** indicate the formation of the $(C_{70}^-)_2$ dimers. SQUID measurements show diamagnetism in **10** in the 1.9−350 K range with the contribution of the Curie impurities < 0.7%. Above 350 K the magnetic moment of the complex increases due to dissociation of dimers. **10** is EPR silent in the 4−285 K range and only <1% of spins from total $C_{70}$ contribute to spin susceptibility (Table 4).

**Peculiarities of the Formation of the $(C_{60}^-)_2$ and $(C_{70}^-)_2$ Dimers in Ionic Complexes.** New complexes of fullerenes $C_{60}$ and $C_{70}$ (**1**−**10**) have an ionic ground state in accordance with redox potentials of donors ($E^{+/0}{}_{1/2} < -0.55$ V), which are more negative than those of fullerenes $C_{60}$ and $C_{70}$ ($E^{0/-}{}_{1/2} = -0.40$−0.44 V).[41] Fullerene radical anions in **1**−**10** tend to dimerize to form the single-bonded $(C_{60}^-)_2$ and $(C_{70}^-)_2$ dimers in contrast to some previously studied ionic complexes ($Cp_2Co{\cdot}C_{60}{\cdot}CS_2$,[4] $Cp_2Co{\cdot}C_{60}{\cdot}C_6H_5CN$,[5] $Cp_2Co{\sim}C_{70}$,[39] and $Cp^*{}_2Ni{\cdot}C_{60}{\cdot}CS_2$[6]). The possible difference between the complexes **1**−**10** and previously studied ones is the use of $C_6H_4Cl_2$ as a solvent instead of $CS_2$ or other solvents. The latter molecules can be inserted between the fullerene spheres[42,43] thus preventing dimerization. As it is shown in Figure 3, $C_6H_4Cl_2$ tends to form columns[18,44] allowing a close approach of the fullerene spheres to each other.

Dimerization of $C_{60}^{\bullet-}$ is reversible with a small hysteresis and affects magnetic properties of the complexes. The single-bonded $(C_{60}^-)_2$ and $(C_{70}^-)_2$ dimers are diamagnetic. It is possible that electron on LUMO of fullerene radical anions participates in the formation of the intercage C−C $\sigma$-bond. The formation of diamagnetic anions was observed previously on the $\sigma$-bonding between the $Co^{II}TPP$ and $C_{60}(CN)_2^{\bullet-}$ radical anions (in this case electrons from LUMO of fullerene and $d_{z^2}$ of $Co^{II}TPP$ participate in the $\sigma$-bonding).[45] Dimerization results in the decrease of the magnetic moments of the complexes and magnetic dilution of the paramagnetic centers ($D^{\bullet+}$) by bulky diamagnetic dimers. As a result, the complexes containing fullerene dimers are either diamagnetic or show a paramagnetic behavior with weak antiferromagnetic interactions of spins at low temperatures. The other consequences of dimerization are a break of exchange coupling between cations and fullerene radical anions observed in a high-temperature monomeric phase, and the appearance of the EPR signals from isolated cations in the low-temperature dimeric phase.

The complexes show a semiconductive behavior with RT conductivity of ~$10^{-5}$−$10^{-2}$ S·cm$^{-1}$ (Table 5). These values

(39) Mrzel, A.; Umek. P.; Cevk, P.; Omerzu, A.; Mihailovic, D. *Carbon* **1998**, *36*, 603−606.
(40) Paul, P.; Bolskar, R. D.; Clark, A. M.; Reed, C. A. *Chem. Commun*. **2000**, 1229−1230.
(41) Dubois, D.; Kadish, K. M.; Flanagan, S.; Haufler, R. E.; Chibante, L. P. F.; Wilson, L. J. *J. Am. Chem. Soc.* **1991**, *113*, 4364−4366.
(42) Konarev, D. V.; Valeev, E. F.; Slovokhotov, Yu. L.; Shul'ga, Yu. M.; Roschupkina, O. S.; Lyubovskaya, R. N. *Synth. Met*. **1997**, *88*, 285−287.
(43) Kveder, V. V.; Steinman, E. A.; Narimbetov, B. Zh.; Khasanov, S. S.; Rozenberg, L. P.; Shibaeva, R. P.; Bazhenov, A. V.; Gorbunov, A. V.; Maksimuk, M. Yu.; Konarev, D. V.; Lyubovskaya R. N.; Ossipyan, Yu. A. *Chem. Phys*. **1997**, *216*, 407−415.
(44) Konarev, D. V.; Khasanov, S. S.; Saito, G.; Vorontsov, I. I.; Otsuka, A.; Lyubovskaya, R. N.; Antipin, Yu. M. *Inorg. Chem*.**2003**, *42*, 3706−3708.
(45) Konarev, D. V.; Khasanov, S. S.; Otsuka, A.; Yoshida, Y.; Saito, G. *J. Am. Chem. Soc*. **2002**, *124*, 7648−7649.

***Table 5.*** RT Conductivity of the Complexes

| N | conductivity, S·cm$^{-1}$ |
|---|---|
| **1** | $6 \times 10^{-5}$ |
| **4** | $8 \times 10^{-4}$ |
| **6** | $2 \times 10^{-5}$ |
| **7** | $2 \times 10^{-2}$ |
| **8** | $2 \times 10^{-2}$ |

***Table 6.*** Temperatures of the Existence of Monomeric and Dimeric Phases in **1**−**10**

$$(D^{\bullet+})_2\cdot[(C_{60(70)} - C_{60(70)})^{2-}]\cdot(Sol)_{2x}\ (T < T_1) \rightleftarrows 2[(D^{\bullet+})\cdot(C_{60(70)}{}^{\bullet-})\cdot(Sol)_x]\ (T > T_2)$$

dimeric phase — monomeric phase

| N | D | $C_{60(70)}$ | sol. | $x$ | $T_1$, K | $T_2$, K |
|---|---|---|---|---|---|---|
| **1** | $Cp^*_2Cr$ | $C_{60}$ | $C_6H_4Cl_2$ | 2 | 200 | 230 |
| **2** | $Cp^*_2Cr$ | $C_{60}$ | $C_6H_6$ | 2 | 160 | 190 |
| **3** | Cs | $C_{70}$ | CTV | 1 | 360 | 390 |
| | | | DMF | 7 | | |
| | | | $C_6H_6$ | 0.75 | | |
| **4** | $Cr(C_6H_6)_2$ | $C_{60}$ | $C_6H_4Cl_2$ | 0.7 | 160 | 240 |
| **5** | $Cr(C_6H_6)_2$ | $C_{60}$ | $C_6H_5CN$ | 1 | 240 | >300 |
| **6** | $Cr(C_6H_6)_2$ | $C_{70}$ | $C_6H_4Cl_2$ | 1 | 250 | >300 |
| **7**[a] | $Cr(C_6H_6)_2$ | $C_{60}$ | - | | >300 | |
| **8** | $Cp_2Co$ | $C_{60}$ | $C_6H_4Cl_2$ | 1 | 250 | 350 |
| **9** | $Cp_2Co$ | $C_{70}$ | $C_6H_4Cl_2$ | 0.5 | >300 | |
| **10** | Cs | $C_{70}$ | DMF | 5 | 350 | >380 |

[a] The formation of another $\sigma$-bonded structure is possible.

are typical for ionic complexes and salts containing fullerene radical anions.[1c]

Temperature ranges of the existence of monomeric and dimeric phases in **1**−**10** are summarized in Table 6. The dissociation temperatures for the $(C_{60}^-)_2$ dimers vary in the 160−250 K range, whereas those for the $(C_{70}^-)_2$ dimers are in the 250−360 K range. The stability of the $(C_{60}^-)_2$ dimers in the solid state depends on donor and solvent molecules involved in the complex. Probably the size of these molecules affects the distances between the fullerene anions in the crystal structure. Indeed, the increase in the distance between the centers of the $C_{60}^-$ spheres from 9.986 Å in $Cr(C_6H_5Me)_2\cdot C_{60}$ (RT)[16,17] up to 10.10 Å in **1** (RT)[18] decreases the dissociation temperature for the $(C_{60}^-)_2$ dimer from 250 down to 200−220 K. Even small variation of the size of solvent molecules ($C_6H_4Cl_2$ and $C_6H_6$ in **1** and **2**, $C_6H_4Cl_2$ and $C_6H_5CN$ in **4** and **5**) with the same donor molecule ($Cp^*_2Cr$ and $Cr(C_6H_6)_2$) shifts the dissociation temperatures by 40−70 K.

The intercage C−C $\sigma$-bond dissociation energies fall into the range of 25−63 kJ·mol$^{-1}$ for the $(C_{60}^-)_2$ dimer in **1**, **2**, **4**, **5**, and **8**. These energies indicate the weakness of these bonds in comparison with the single C−C bond, for example, in $CH_3-CH_3$ (the dissociation energy is 368 kJ·mol$^{-1}$).[46] The intercage C−C bonds in the $(C_{60}^-)_2$ and $(C_{70}^-)_2$ dimers of 1.597(7)[18] and 1.584(9) Å[19] are also noticeably longer than the single C−C bond between sp$^3$ carbons (1.541(3) Å).[47]

The $(C_{70}^-)_2$ dimer is more stable than the $(C_{60}^-)_2$ one. This is manifested in the shorter intercage C−C bond according to the X-ray diffraction data (1.584(9) Å in **3**[19] *vs* 1.597(7) Å in **1**[18]) and higher temperature of the beginning of dissociation (250−360 K vs 160−250 K, respectively (Table 6)). Dimer stability is defined mainly by the on-site Coulomb repulsive energy between fullerene anions. Because of this, the extended $\pi$-system of $C_{70}^-$ stabilizes the $C_{70}^-$ dimeric state relative to that of $C_{60}^-$. The presence of two negative charges on the $(C_{60}^-)_2$ dimer also substantially destabilized this dimer relative to isoelectronic neutral single-bonded $(C_{59}N)_2$ dimer formed by azofullerene. According to the data of Prassides et al.,[15b] the $(C_{59}N)_2$ dimer begins to dissociate above 500 K and even at 740 K only 1 of every ~6000 dimers is cleaved into monomeric fragments.

Both $(C_{60}^-)_2$ and $(C_{70}^-)_2$ dimers have characteristic IR and NIR spectra, which allow them to be identified in ionic complexes. Numerous additional bands observed in the IR spectra (see the Supporting Information) were attributed to the lowering of the symmetry of fullerenes in a dimer. Two or even three bands appear in the NIR spectra as a result of dimerization of fullerene radical anions (Figures 8b and 9b). The additional band can be associated with interfullerene electronic transitions within one dimer. Similarly, additional bands were observed in the spectrum of the $\sigma$-bonded ($Co^{II}TPP\cdot C_{60}(CN)_2^-$) anion, one of which was ascribed to the transition between $Co^{II}TPP$ and $C_{60}(CN)_2^-$ in the $\sigma$-bonded unit.[45]

## Conclusion

In summary, we have shown the formation of diamagnetic single bonded $(C_{60}^-)_2$ and $(C_{70}^-)_2$ dimers in ionic complexes of fullerenes $C_{60}$ and $C_{70}$. Dimerization is realized as reversible phase transitions and results in the changes in structural and magnetic properties of the complexes. Peculiarities of the $(C_{60}^-)_2$ and $(C_{70}^-)_2$ dimeric phases have been studied. It has been shown that the $(C_{70}^-)_2$ dimers are more stable than the $(C_{60}^-)_2$ ones and dimer stability depends on donor and solvent molecules involved in the complex. The IR and UV−vis−NIR spectra of the dimers are useful tools for their identification.

## Experimental Section

**Materials.** $Cp^*_2Cr$, $Cp_2Co$, and $Cp_2Cr$ were purchased from Aldrich. $Cr^0(C_6H_6)_2$ was purchased from Strem Chemicals. $C_{60}$ and $C_{70}$ of 99.98 and 99.0% purity, respectively were purchased from MTR Ltd.. Solvents were purified in argon atmosphere. *o*-Dichlorobenzene ($C_6H_4Cl_2$) was distilled over $CaH_2$. Toluene ($C_6H_5Me$), benzene ($C_6H_6$) and hexane were distilled over Na/benzophenone. Benzonitrile ($C_6H_5CN$) was distilled over Na/benzophenone. *N*,*N*-dimethylformamide (DMF) of HPLC grade (Aldrich) was distilled under reduced pressure. The solvents were degassed and stored in a glove box. All manipulations with **1**−**10** were carried out in a MBraun 150B−G glove box with controlled atmosphere and the content of $H_2O$ and $O_2$ less than 1 ppm. The samples were stored in a glove box and were sealed in 2 mm quartz tubes for EPR and SQUID measurements under $10^{-5}$ Torr. KBr pellets for IR and UV−vis−NIR measurements were prepared in the glove box.

**General.** UV−vis−NIR spectra were measured on a Shimadzu UV-3100 spectrometer in the 240−2600 nm range. FT-IR spectra were measured in KBr pellets with a Perkin-Elmer Paragon 1000 FT−IR spectrometer (400−7800 cm$^{-1}$). A Quantum Design MPMS-XL SQUID magnetometer was used to measure static susceptibilities down to 1.9 K. A sample holder contribution and core temperature independent diamagnetic

(46) Benson, S. W. *J. Chem. Ed.* **1965**, *42*, 502−508.
(47) Kennard, O. In *CRC Handbook of Chemistry and Physics*; Weast, R. C., Ed.; CRC Press: Boca Raton, Florida, 1987; p F106.

susceptibility ($\chi_0$) were subtracted from the experimental values. The values of $\chi_0$ for **6**, **7**, **8** (in the 2−250 K range), and **10** were calculated from the high-temperature range with the appropriate formula: $\chi_M = C/(T - \Theta) + \chi_0$. The $\chi_0$ values for **1**, **2**, **4**, and **5** were calculated using the Pascal constants: −2.3, − 1.41, −0.83, $-0.54 \times 10^{-4}$ emu $mol^{-1}$ for $Cp^*_2Cr$,[48] $Cr^0(C_6H_6)_2$,[49] $C_6H_4Cl_2$, and $C_6H_6$, respectively. The contribution of fullerenes to total susceptibility were ignored because of diamagnetic and paramagnetic components canceled out.[50] EPR spectra were recorded down to 4 K with a JEOL JES-TE 200 X-band ESR spectrometer equipped with JEOL ES-CT470 cryostat. Conductivity was measured by the two-probe technique in a glovebox. The intercage C−C $\sigma$ bond dissociation energy was calculated from the slope of the dependency ln $k$ *vs* 1/$T$. The equilibrium constants ($k = [C_{60}^{\bullet -}]^2/[(C_{60}-C_{60})^{2-}]$ of the reaction: $[\{(C_{60})_2\}^{2-}] \rightleftarrows 2[C_{60}^{\bullet -}]$ were estimated using data of magnetic measurements.

**Synthesis.** Diffusion was carried out in a glass tube of 1.5 cm in diameter and 40 mL volume with a ground glass plug during 1 month. The solvent was decanted and the crystals were washed with hexane and dried. The composition of the compounds was determined from the X-ray diffraction on a single crystal for **1** and **3**, and by the elemental analysis for **2**, **4**−**10** (Table 2). In **2**, and **4**−**10** the difference (100-%(C, H, Cl, N)) exceeds the calculated content of metals (Co and Cr) indicating the addition of oxygen to the complexes during the elemental analysis. Indeed, all complexes are air sensitive. Oxidation may be realized, for example, through the addition of oxygen to the fullerene radical anion: $(\text{fullerene})^{\bullet -} + O_2 \rightarrow (\text{fullerene}\cdot O_2^-)$. The addition of approximately one $O_2$ molecule per one formula unit of the complex is observed. Thus, the calculated C, H, N, and Cl (%) content was corrected for the following composition (Formula unit:$O_2$). We assume that oxygenation occurring during elemental analysis is extrinsic and omit oxygen through the manuscript. Previously, the addition of $O_2$ to $C_{60}$ ionic complexes during elemental analysis was also reported.[3,51] The shape and color of the crystals of the compounds are given in Table 2.

The crystals of **2** were obtained by diffusion of hexane (20 mL) in the $C_6H_5CN/C_6H_6$ solution (1/4) (20 mL) containing $C_{60}$ (20 mg, 0.028 mmol) and $Cp^*_2Cr$ (9 mg, 0.028 mmol) (70% yield).

The crystals of **5** were obtained by diffusion of hexane (20 mL) in the $C_6H_5CN/C_6H_6$ solution (1/4) (20 mL) containing $C_{60}$ (20 mg, 0.028 mmol) and $Cr(C_6H_6)_2$ (12 mg, 0.056 mmol). The crystals of two different shapes were formed and were separated under microscope giving **5** as well shaped black parallelepipeds (40% yield) together with black elongated plates (20% yield).

The crystals of **4** and **6** were prepared by diffusion of hexane (20 mL) in $C_6H_4Cl_2$ (20 mL) containing $C_{60}$ (20 mg, 0.028 mmol) (**4**) or $C_{70}$ (20 mg, 0.024 mmol) (**6**) and $Cr(C_6H_6)_2$ (12 mg, 0.056 mmol). After 1 month polycrystalline **4** and **6** (50−70% yield) were obtained.

Polycrystalline **7** was obtained by mixing filtered $C_6H_6$ (30 mL) or $C_6H_5Me$ (25 mL) solution containing $C_{60}$ (20 mg, 0.028 mmol) with that (5 mL) containing $Cr(C_6H_6)_2$ (12 mg, 0.056 mmol). After 24 h, the colorless solution was filtered and the precipitate was washed with benzene and dried. The IR spectra and the elemental analyses of the products obtained from $C_6H_6$ and $C_6H_5Me$ were identical and showed the absence of solvent molecules in the complex.

Polycrystalline **8** was obtained by mixing hot filtered $C_6H_4Cl_2$ solutions containing $C_{60}$ (20 mg, 0.028 mmol) in 20 mL and $Cp_2Co$ (6.3 mg, 0.033 mmol) in 5 mL. 20 mL of hexane was layered over the obtained solution in a 50 mL flask. After 4 d, the solution was decolorized and black small crystals were crystallized (80% yield).

Polycrystalline **9** was obtained by diffusion of hexane in $C_6H_5CN/C_6H_4Cl_2$ solution (1/4) (20 mL) containing $C_{70}$ (20 mg, 0.024 mmol) and $Cp_2Co$ (6.3 mg, 0.033 mmol) (70% yield).

The $(Cs^+)\cdot(C_{70}^{\bullet -})$ salt was generated in solution on dissolving $C_{70}$ (20 mg, 0.024 mmol) and cesium (3.5 mg, 0.0264 mmol) in 2 mL of DMF. **10** was crystallized during diffusion of hexane (20 mL) in the solution of $(Cs^+)\cdot(C_{70}^{\bullet -})$ in $C_6H_6$/DMF (9/1) the (50% yield).

**Abbreviation in the Text.** TDAE: tetrakis(dimethylaminoethylene); $Cp_2Co$: bis(cyclopentadienyl)cobalt (II); $Cp_2Cr$: bis(cyclopentadienyl)chromium; $Cr(C_6H_6)_2$: bis(benzene)chromium (0); $Cr(C_6H_5Me)_2$; bis(toluene)chromium (0); $Cp^*_2Ni$: bis(pentamethylcyclopentadienyl)nickel (II); $Cp^*_2Cr$: bis(pentamethylcyclopentadienyl)chromium; $Cr^{III}TPP$: 5, 10, 15, 20-tetraphenylporphyrin chromium (III); $PPN^+$: bis(triphenylphosphoranylidene)ammonium; $Co^{II}TPP$: 5, 10, 15, 20- tetraphenylporphyrinate cobalt (II); $Ph_4P^+$: tetraphenylphosphonium; CTV: cyclotriveratrylene; THF: tetrahydrofuran; DMF: *N*,*N*-dimethylformamide; $C_6H_6$: benzene; $C_6H_4Cl_2$: *o*-dichlorobenzene; $C_6H_5Me$: toluene; $C_6H_5CN$:benzonitrile; $CH_3CN$: acetonitrile.

**Acknowledgment.** The work was supported by the COE Research on Elements Science No. 12CE2005, JSPS, and the RFBR Grant No. 03-03-32699a.

**Supporting Information Available:** Crystallographic data of **1** at 300 and 100 K (CIF files) and IR spectra of **1**-**10**. This materials is available free of charge via Internet at http://pubs.acs.org.

JA035546A

(48) Gebert, E.; Reis, A. H.; Miller, J. S.; Rommelmann, H.; Epstein, A. J. *J. Am. Chem. Soc.* **1982**, *104*, 4403−4410.
(49) Miller, J. S.; O'Hare, D. M.; Chakraborty, A.; Epstein, A. J. *J. Am. Chem. Soc*. **1989**, *111*, 7853−7860.
(50) (a) Haddon, R. C.; Schneemeyer, L. F.; Waszczak, J. V.; Glarum, S. H.; Tycko, R.; Dabbagh, G.; Kortan, A. R.; Muller, A. J.; Mujsce, A. M.; Rosseinsky, M. J.; Zahurak, S. M.; Makhija, A. V.; Thiel, F. A.; Raghavachari, K.; Cockayne, E.; Elser, V. *Nature* **1991**, *350*, 46−47. (b) Luo, W.; Wang, H.; Ruoff, R.; Cioslowski, J.; Phelps, S. *Phys. Rev. Lett.* **1994**, *73*, 186−188.
(51) Kitagawa, T.; Lee Y.; Takeuchi, K. *Chem. Commun*. **1999**, 1529−1530.